Available online at www.sciencedirect.com
ScienceDirect
Automatica 44 (2008) 15–27
automatica
www.elsevier.com/locate/automatica

Performance of convergence-based variable-gain control of optical storage drives☆

N. van de Wouw[a,*], H.A. Pastink[b], M.F. Heertjes[c], A.V. Pavlov[d], H. Nijmeijer[a]

[a] *Department of Mechanical Engineering, Eindhoven University of Technology, P.O. Box 513, 5600 MB Eindhoven, The Netherlands*
[b] *Océ Technologies, P.O. Box 101, 5900 MA, Venlo, The Netherlands*
[c] *Philips Applied Technologies, Department Mechatronics Technologies, 5600 MD Eindhoven, The Netherlands*
[d] *NTNU, Department of Engineering Cybernetics, N7491 Trondheim, Norway*

Received 1 September 2005; received in revised form 28 January 2007; accepted 18 April 2007
Available online 20 August 2007

Abstract

In this paper, a method for the performance assessment of a variable-gain control design for optical storage drives is proposed. The variable-gain strategy is used to overcome well-known linear control design trade-offs between low-frequency tracking properties and high-frequency noise sensitivity. A convergence-based control design is proposed that guarantees stability of the closed-loop system and a unique bounded steady-state response for any bounded disturbance. These favourable properties, guaranteed by virtue of convergence, allow for a unique performance evaluation of the control system. Moreover, technical conditions for convergence are derived for the variable-gain controlled system and a quantitative performance measure, taking into account both low-frequency tracking properties and high-frequency measurement noise sensitivity, is proposed. The convergence conditions together with the performance measure jointly constitute a design tool for tuning the parameters of the variable-gain controller. The resulting design is shown to outperform linear control designs.

Keywords: Optical storage drives; Variable-gain control; Convergent systems; Performance assessment

1. Introduction

Optical storage drives, such as CD or DVD, either ROM or audio, drives, are generally controlled using linear (PID-type) control strategies. Especially for portable or automotive applications, the requirements on the control design relate to both tracking requirements and disturbance attenuation properties. In this scope, two types of disturbances can be distinguished. Firstly, low-frequent shock disturbances are inevitable in automotive applications due to engine vibration or road excitation. Secondly, high-frequent disturbances are due to the fact that the measurement of the position of the disc tracks relative to the lens position, by the optical pick-up unit, is corrupted by the presence of finger prints, scratches and dirt spots (i.e. disc defects).

When applying linear control, the following fundamental design trade-off is inherently present: increasing the closed-loop bandwidth improves the low-frequency disturbance rejection properties at the cost of deteriorating the sensitivity to high-frequency measurement noise (Freudenberg, Middleton, & Stefanopoulou, 2000). Nonlinear control, or more specifically, nonlinear PID control, see also the work of Armstrong, Neevel, and Kusid (2001), Jiang and Gao (2001), Fromion and Scorletti (2002) and Armstrong, Gutierrez, Wade, and Joseph (2006) combines the possibility of having increased performance in terms of shock attenuation without unnecessarily deteriorating the time response under disc defect disturbances. In Heertjes and Steinbuch (2004) and Heertjes, Pastink, van de Wouw, and Nijmeijer (2006), variable-gain control strategies are proposed to overcome the practical implications of such design limitations. In those papers, the comparison between control designs is based on time- and frequency-domain simulations and experiments. Such analyses do not directly support a quantitative comparison of the performance of different variable-gain and

☆ This paper was not presented at any IFAC meeting. This paper was recommended for publication in revised form by Associate Editor Masaki Yamakita under the direction of Editor Mituhiko Araki.

* Corresponding author.
E-mail address: n.v.d.wouw@tue.nl (N. van de Wouw).

0005-1098/$ - see front matter © 2007 Elsevier Ltd. All rights reserved.
doi:10.1016/j.automatica.2007.04.004

linear control designs. On the other hand, the power of linear control strategies lies in the fact that essential closed-loop properties, such as stability and performance, can readily be checked. It should be noted that generally the design of nonlinear control systems is merely aiming at closed-loop stability and the performance assessment is confined—if present at all—to simulation-based reasoning.

For linear control systems, frequency-domain analysis plays a central role in the performance assessment of these systems. Such analysis hinges on the fact that an asymptotically stable linear time-invariant system exhibits a *unique* bounded steady-state solution for any bounded disturbance. Nonlinear systems do generally not exhibit such properties. Instead, perturbed nonlinear systems can exhibit multiple steady-state solutions. These facts seriously hamper a performance analysis of such nonlinear control systems. The class of *convergent* systems, however, exhibits such favourable properties; see Demidovich (1967), Pavlov, Pogromsky, van de Wouw, and Nijmeijer (2004) and Pavlov, van de Wouw, and Nijmeijer (2005) for more information on the notion of convergence.

Convergence implies stability (of an equilibrium point) in the absence of disturbances and it guarantees the existence of a *unique* bounded globally asymptotically stable steady-state solution for every bounded disturbance. Obviously, if such a solution does exist, all other solutions, regardless of their initial conditions, converge to this solution, which can be considered as a steady-state solution (Demidovich, 1967; Pavlov et al., 2004). Similar notions describing the property of solutions converging to each other are studied in literature. The notion of contraction has been introduced in Lohmiller and Slotine (1998) (see also references therein). An operator-based approach towards studying the property that all solutions of a system converge to each other is pursued in Fromion, Monaco, and Normand-Cyrot (1996) and Fromion, Scorletti, and Ferreres (1999). In Angeli (2002), a Lyapunov approach has been developed to study the global uniform asymptotic stability of all solutions of a system (in Angeli, 2002, this property is called incremental stability).

We propose a variable-gain control design, which ensures convergence (and therefore stability) of the closed-loop system, and therefore allows for a unique performance evaluation in the face of disturbances. Still, a definition of a performance measure is needed for a quantitative comparison of control designs. We propose such a performance measure and use it to support a performance-based control design for variable-gain controlled optical storage drives. It will be shown that stability-based and performance-based control synthesis may lead to different designs and that the variable-gain strategy can outperform linear control strategies. In Fromion et al. (1999) and Fromion and Scorletti (2002), the concept of incremental stability is used to assess the performance of nonlinear control systems. The performance is studied by investigating the $\mathscr{L}_2$-norms of inputs and outputs of the control system. This approach is less suitable for the performance assessment for optical storage drives because the performance of such systems is closely related to the $\mathscr{L}_\infty$-norm of the tracking error since that determines whether the disc read-out is terminated or not. Moreover, a view on performance based on gains between norms on inputs and outputs can be a rather conservative one. Therefore, we adopt the perspective of exactly computing the steady-state responses (which are unique by virtue of the convergence property) to disturbances from the specific class of harmonic disturbances and defining the control performance on the basis of these quantitative data. The performance in the face of harmonic disturbances is specifically important for optical storage drives. For example, in practice the performance is tested experimentally by constructing so-called 'drop-out-level curves' (Heertjes, Cremers, Rieck, & Steinbuch, 2005), which show the level of the harmonic disturbance for which a termination of the disc read-out occurs for varying disturbance frequencies.

The paper is organised as follows. In Section 2, the optical storage drive is introduced and a simple model for the dynamics (in radial direction) is proposed. Moreover, a conventional linear control design and the related fundamental design limitations are discussed. The variable-gain control strategy is introduced in Section 3. Section 4 introduces the class of convergent systems and proposes conditions for convergence. Subsequently, the closed-loop behaviour is studied both in the time domain and in the frequency domain in Section 5. In Section 6, the performance measure is introduced and used to discriminate between different control designs. Finally, a discussion of the obtained results and concluding remarks are given in Section 7.

2. Modelling and control of optical storage drives

Optical storage drives obtain information from a disc using the principles of optical read-out. Hereby, information is stored on the disc's surface by means of a sequence of reflective lands and non-reflective pits contained in a track. The information is read from the disc via a light path guided by a lens in a so-called optical pick-up unit. The light is reflected by the pit and land structure on the disc. We focus on the control of the lens in radial direction. The tolerance on the tracking to be preserved in playing is dictated by the track width which amounts 0.74 μm for a DVD. A model for the lens dynamics in radial direction is depicted schematically in Fig. 1. Herein, r represents the position of the track to be read, since the turntable with the disc is mounted on the base frame. The two-stage control strategy of the optical pick-up unit consists of a so-called long-stroke motion of a sledge containing the lens (p_{ls}) and a short-stroke motion of the lens with respect to the sledge (p_{ss}). We primarily focus on the control of the short-stroke motion (i.e. p_{ls} is assumed fixed). The lens dynamics in the

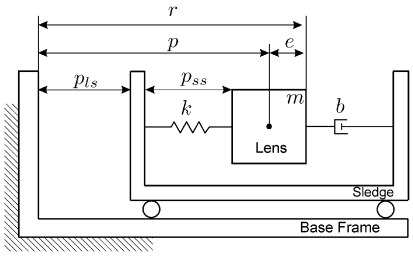

Fig. 1. Model of the dynamics in radial direction.

sledge are modelled by a mass–spring–damper system with mass m, stiffness k and damping b.

A block-diagram of a linearly controlled optical storage drive is given in Fig. 2. Herein, n represents measurement noise and u is the control action. It should be noted that in optical storage drives the error e (the difference between disk position r and the actual lens position p) is the measured variable. Since it is corrupted by the measurement noise it is denoted by $\tilde{e}$. Moreover, $H_P(s)$ represents the transfer function related to the lens dynamics and actuator dynamics:

$$H_P(s) = \frac{p(s)}{u(s)} = \frac{\omega_a}{(ms^2 + bs + k)(s + \omega_a)}, \quad s \in \mathbb{C}.$$

Note that the actuator dynamics are modelled using a low-pass filter, where ω_a is the breakpoint of the filter. This low-pass characteristic is due to the actuator inductance from voltage to current, see Bittanti, Dell'Orto, Di Carlo, and Savaresi (2002). The transfer function $H_C(s)$ representing the PID-controller satisfies

$$H_C(s) = \frac{u(s)}{\tilde{e}(s)} = \frac{k_p\omega_{lp}^2(s^2 + (\omega_d + \omega_i)s + \omega_d\omega_i)}{\omega_d(s^3 + 2\beta\omega_{lp}s^2 + \omega_{lp}^2 s)},$$

where ω_i is the breakpoint of the integral action, ω_d is the breakpoint of the differential action, ω_{lp} and β denote the breakpoint and the damping parameter of the low-pass filter, respectively, and k_p is a gain. The parameter values related to the lens dynamics, actuator dynamics and the control design for a typical DVD player are $m = 7.0 \times 10^{-4}$ kg, $k_p = 9.0 \times 10^3$ N/m, $b = 2.0 \times 10^{-2}$ Ns/m, $\omega_i = 1.3 \times 10^3$ rad/s, $k = 32.2$ N/m, $\omega_d = 1.8 \times 10^3$ rad/s, $\omega_a = 1.3 \times 10^5$ rad/s, $\omega_{lp} = 2.8 \times 10^4$ rad/s and $\beta = 0.7$, see Heertjes et al. (2005, 2006) for related experimental validation results.

The issue of disturbance modelling will be addressed in more detail in Section 6. It should be noted that we consider two types of disturbances denoted by r and n. The position of the disc track, r, is considered as a disturbance since the disc is (rigidly) attached to the turntable of the optical storage drive, which vibrates due to external disturbances. The servo-error e is measured through a reconstruction mechanism using a so-called extended S-curve (Stan, 1998) and n is the related measurement noise. The low-frequency disturbances r typically occur in a frequency range of 10–200 Hz and the high-frequency disturbances typically have a frequency content between 3–45 kHz.

In such linearly controlled motion systems, increasing the gain k_p results in improved tracking performance and disturbance rejection in the low-frequency range. However, at the same time the disturbance rejection properties in the high-frequency range deteriorate.The latter represents a fundamental design trade-off in linear control design. In order to overcome such fundamental design limitations, in Heertjes and Sperling (2003) and Heertjes and Steinbuch (2004) variable-gain strategies are proposed.

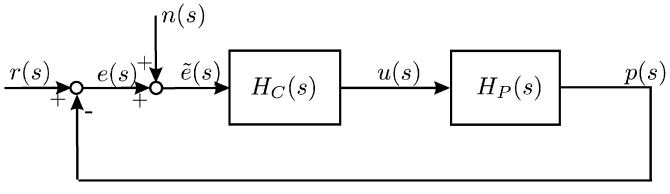

Fig. 2. Block diagram of a linearly controlled optical storage drive.

3. Variable-gain control design

The basic idea behind the variable-gain control design is that, firstly, when the error is small a low-gain design should be in effect to ensure low sensitivity to high-frequency measurement noise and, secondly, when the error becomes large due to low-frequency shocks a high-gain design should be active to ensure a high level of low-frequency tracking performance. In Fig. 3, the variable gain strategy is depicted schematically. It differs from Fig. 2 through the addition of the variable-gain element $\phi(\tilde{e}) = (\alpha - \alpha\delta/\ |\ \tilde{e}\ |)H(|\ \tilde{e}\ | - \delta)$, with $H(\cdot)$ the Heaviside function. Herein, the control design parameters $\alpha \geqslant 0$ and $\delta \geqslant 0$ represent the additional gain and a dead zone length, respectively. The variable gain $\phi(\tilde{e})$ and the output of the variable gain block $\gamma(\tilde{e}) = \phi(\tilde{e})\tilde{e} =: \alpha\varepsilon(\tilde{e})[\tilde{e} - \delta\text{sign}(\tilde{e})]$ are depicted in Fig. 4.

For the stability analysis, a state-space notation will be adopted for the feedback loop shown in Fig. 3:

$$\dot{x} = Ax + B\gamma(\tilde{e}) + Bq(t), \quad \tilde{e} = q(t) - Cx, \tag{1}$$

with $q(t) = r(t) + n(t) \in \mathbb{R}$, the state vector $x \in \mathbb{R}^6$, the measured radial error signal $\tilde{e} \in \mathbb{R}$ and the scalar nonlinearity $\gamma(\tilde{e})$ due to the variable-gain element. The state x in system (1)

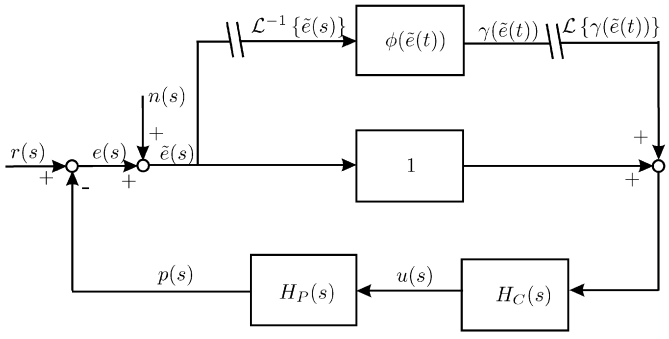

Fig. 3. Block diagram of a variable-gain controlled optical storage drive.

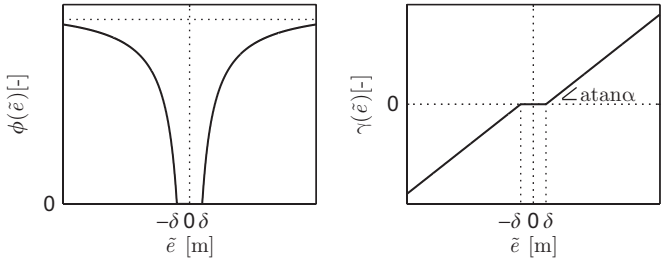

Fig. 4. Variable gain $\phi(\tilde{e})$ and the output of the variable gain block $\gamma(\tilde{e})$.

is defined as

$$x = [x_1 \;\; x_2 \;\; x_3 \;\; x_4 \;\; x_5 \;\; x_6]^{\mathrm{T}}$$

$$= \left[\omega_d \tilde{D} \;\; \frac{1}{1+\omega_i/\omega_d}\tilde{P} \;\; \frac{1}{\omega_i}\tilde{I} \;\; F \;\; p \;\; \dot{p}\right]^{\mathrm{T}}.$$

The variables x_1, x_2 and x_3 correspond to the derivative, proportional and integral action of the PID controller, all filtered by the low-pass filter installed in series with the PID controller; x_4 denotes the force that actuates the lens mass; x_5 and x_6 represent the radial position and the radial velocity of the lens mass, respectively. In (1), $C = [0 \;\; 0 \;\; 0 \;\; 0 \;\; 1 \;\; 0]$,

$$A = \begin{bmatrix} -2\beta\omega_{lp} & -\omega_{lp}^2 & 0 & 0 & -k_p\omega_{lp}^2 & 0 \\ 1 & 0 & 0 & 0 & 0 & 0 \\ 0 & 1 & 0 & 0 & 0 & 0 \\ \dfrac{\omega_a}{\omega_d} & \omega_a\left(1+\dfrac{\omega_i}{\omega_d}\right) & \dfrac{\omega_a}{\omega_i} & -\omega_a & 0 & 0 \\ 0 & 0 & 0 & 0 & 0 & 1 \\ 0 & 0 & 0 & \dfrac{1}{m} & -\dfrac{k}{m} & -\dfrac{b}{m} \end{bmatrix}$$

and $B = [k_p\omega_{lp}^2 \;\; 0 \;\; 0 \;\; 0 \;\; 0 \;\; 0]^{\mathrm{T}}$. Since the disturbances $r(t)$ and $n(t)$ enter the system as $r(t) + n(t)$, for stability analysis of the closed-loop system they are merged into one signal $q(t) := r(t) + n(t)$.

In stability analysis of the closed-loop system we are interested in the following question: under what conditions on the controller parameters do all solutions of the closed-loop system (1) corresponding to a bounded input signal $q(t)$ converge to a unique bounded steady-state solution? This property of the closed-loop system—the so-called convergence property—as well as an answer to the above stated question are discussed in the next section.

4. Convergent systems

In this section we give a definition of convergent systems, discuss some properties of such systems and provide sufficient conditions under which a system of the form (1) is convergent. Consider the system

$$\dot{x} = f(x, w(t)), \tag{2}$$

with state $x \in \mathbb{R}^n$, piecewise-continuous input $w : \mathbb{R} \to \mathbb{R}^m$ and locally Lipschitz function $f(x, w)$.

Definition 1 (*Demidovich (1967) and Pavlov et al. (2004)*). System (2) with a given input $w(t)$ is said to be (*exponentially*) *convergent* if

i. all solutions $x(t)$ are well-defined for all $t \in [t_0, \infty)$ and all initial conditions $t_0 \in \mathbb{R}$, $x(t_0) \in \mathbb{R}^n$;
ii. there exists a unique solution $\bar{x}_w(t)$ defined and bounded for all $t \in (-\infty, \infty)$;
iii. the solution $\bar{x}_w(t)$ is globally (exponentially) asymptotically stable.

The solution $\bar{x}_w(t)$ is called a *steady-state solution*. As follows from the definition of convergence, any solution of a convergent system "forgets" its initial condition and converges to some steady-state solution $\bar{x}_w(t)$ which is determined only by the input $w(t)$. Moreover, if the input $w(t)$ is periodic with period T, then the corresponding steady-state solution $\bar{x}_w(t)$ is also periodic with the same period T, see Demidovich (1967) and Pavlov et al. (2005).

For systems of the form (note that this form conforms with (1))

$$\dot{x} = Ax + B\sigma(y) + w_1(t), \quad y = w_2(t) - Cx, \tag{3}$$

with state $x \in \mathbb{R}^n$, input $w = [w_1^{\mathrm{T}}, w_2]^{\mathrm{T}} \in \mathbb{R}^{n+1}$ and scalar nonlinearity $\sigma(y)$ depending on the scalar output y, the exponential convergence property can be verified with the following result.

Theorem 1. *Consider system* (3). *Suppose the matrix A is Hurwitz and the nonlinearity* $\sigma(y)$ *satisfies the incremental sector condition*

$$0 \leqslant \frac{\sigma(y_1) - \sigma(y_2)}{y_1 - y_2} \leqslant \mu \quad \forall y_1, y_2 \in \mathbb{R} | y_1 - y_2 \neq 0, \tag{4}$$

where $\mu \in [0, \infty)$. *If the system satisfies the condition*

$$\Re\{G(\mathrm{j}\omega - \lambda)\} > -\frac{1}{\mu} \quad \forall \omega \in \mathbb{R}, \tag{5}$$

for some $\lambda \geqslant 0$, *where* $G(s) := C(sI - A)^{-1}B$, *then system* (3) *is exponentially convergent for any bounded piecewise-continuous input* $w(t)$. *Moreover, the steady-state solution is globally exponentially stable with an exponent* $\tilde{\lambda}$ *satisfying* $\tilde{\lambda} > \lambda$, *i.e. it holds that*

$$\|\bar{x}_w(t) - x(t)\| \leqslant \beta e^{-\tilde{\lambda}(t-t_0)} \|\bar{x}_w(t_0) - x(t_0)\| \quad \forall t > t_0, \tag{6}$$

for some $\beta > 0$ *independent of the particular input* $w(t)$.

Proof. For the case that $w_2(t) \equiv 0$ this theorem was proved in Yakubovich (1964). For the case that $w_2(t) \not\equiv 0$, notice that for all $x_1, x_2 \in \mathbb{R}^n$ such that $Cx_1 - Cx_2 \neq 0$ the time-varying nonlinearity $\sigma(w_2(t) - Cx)$ satisfies

$$\frac{\sigma(w_2(t) - Cx_1) - \sigma(w_2(t) - Cx_2)}{-Cx_1 + Cx_2} = \frac{\sigma(w_2(t) - Cx_1) - \sigma(w_2(t) - Cx_2)}{(w_2(t) - Cx_1) - (w_2(t) - Cx_2)}.$$

Therefore, by condition (4) we obtain

$$0 \leqslant \frac{\sigma(w_2(t) - Cx_1) - \sigma(w_2(t) - Cx_2)}{-Cx_1 + Cx_2} \leqslant \mu$$
$$\forall t \in \mathbb{R}, \;\; x_1, x_2 \in \mathbb{R}^n | Cx_1 - Cx_2 \neq 0. \tag{7}$$

Once condition (7) is established, the proof of exponential convergence and inequality (6) repeats the proof from Yakubovich (1964) for the case of $w_2(t) \equiv 0$. □

Notice, that the closed-loop system (1) is in the form (3) with $y = \tilde{e}$, $\sigma(y) = \gamma(\tilde{e})$, $w_1(t) = Bq(t)$ and $w_2(t) = q(t)$. One

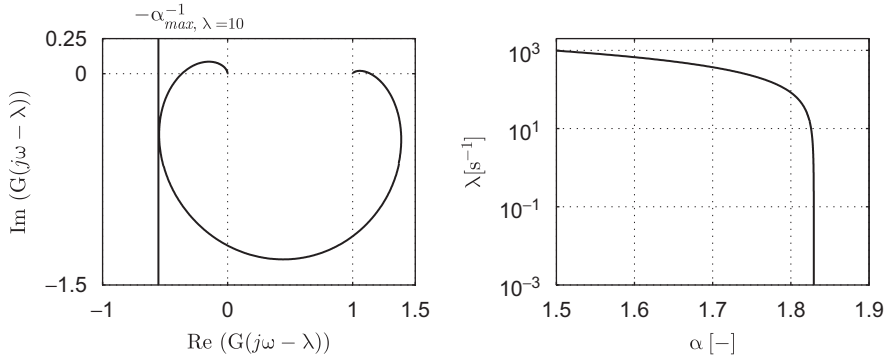

Fig. 5. Left: Nyquist plot of $G(\mathrm{j}\omega-\lambda)$ for $\lambda=10$, and graphical investigation of frequency-domain condition (5). Right: relation between α and the maximum level of λ when condition (5) is satisfied.

can easily verify (see Fig. 4) that the nonlinearity γ satisfies the incremental sector condition

$$0\leqslant\frac{\gamma(\tilde{e}_1)-\gamma(\tilde{e}_2)}{\tilde{e}_1-\tilde{e}_2}\leqslant\alpha\quad\forall\tilde{e}_1,\tilde{e}_2\in\mathbb{R}|\tilde{e}_1-\tilde{e}_2\neq 0,\tag{8}$$

with $\alpha\in[0,\infty)$ representing the additional gain. Moreover, the system matrix A is Hurwitz. In order to guarantee the exponential convergence property, we require that system (1) satisfies the following condition:

$$\Re\{C((\mathrm{j}\omega-\lambda)I-A)^{-1}B\}>-\frac{1}{\alpha},\quad\forall\omega\in\mathbb{R},\tag{9}$$

for some $\lambda\geqslant 0$ and for the matrices A, B and C defined in Section 3. This condition allows for a graphical investigation. The left part of Fig. 5 displays the Nyquist plot of $G(\mathrm{j}\omega-\lambda)$ for $\lambda=10$. Condition (5) is satisfied if the Nyquist plot of $G(\mathrm{j}\omega-\lambda)$ is entirely on the right side of the line l vertically passing through $-1/\alpha$. Hence, α can be increased up to the value at which l is just tangent to the Nyquist plot of $G(\mathrm{j}\omega-\lambda)$. For system (1), in case $\lambda=10$, α is restricted to a maximum value of $\alpha_{\max}=1.82$. Condition (5) is fulfilled for various combinations of α and λ. The right part of Fig. 5 depicts a curve in the (α,λ) space, which establishes what *maximum* value of λ can be assured if condition (5) is satisfied, given a particular value of α. The latter curve indicates a convergence (and thereby stability) region just like the Nyquist plot in the left part of Fig. 5. Namely, for all α on the left side of the vertical asymptote at $\alpha\approx 1.82$, condition (5) is satisfied. In this context it is important to note that λ is a lower bound for the exponential convergence rate of the solutions to the steady-state solution. Clearly, the right part of Fig. 5 expresses the fact that increasing α yields a lower guaranteed exponential convergence rate λ, which also constitutes a trade-off in terms of the transient response of the control system.

Finally, by Theorem 1 we conclude that if the additional gain $\alpha\in[0,1.82)$ then the closed-loop system (5) is exponentially convergent with the rate of exponential convergence λ satisfying $\lambda\geqslant 10$. Notice, that δ does not affect the exponential convergence property provided that $\alpha\in[0,1.82)$. Therefore, from the convergence point of view $\delta\geqslant 0$ can be chosen such that improved performance of the closed-loop system is attained.

It should be noted that a bound on the state (and thus on the error and position of the lens) can be computed, given bounds on the disturbances, based on Theorem 1, see Yakubovich (1964). The proof of this theorem is based on the fact that under the conditions of the theorem there exists a quadratic Lyapunov function for the unperturbed system of the form: $V=x^{\mathrm{T}}Px$, with $P=P^{\mathrm{T}}>0$. Given such matrix P an ultimate bound for the state of the perturbed system can be formulated. Hereto, we define the set

$$\mathscr{E}=\left\{x|\|x\|_P\leqslant\frac{1}{\lambda}\sup_{t\in\mathbb{R}}\|B\gamma(q(t))+Bq(t)\|_P\right\},\tag{10}$$

where $\|x\|_P=\sqrt{x^{\mathrm{T}}Px}$ is called the P-norm of x. The set $\mathscr{E}$ is a positively invariant set and all solutions of the perturbed system starting outside this set will converge to it. Therefore, given bounds on the disturbances $q(t)$ a bound on the P-norm of x is provided.

For practical implementations, it is important to note that the convergence property is robust for model uncertainties if one chooses the additional gain α below α_{max}. The ultimate choice for α is based on both robustness and performance considerations. The desired level of robustness is attained by choosing $\alpha_{max}-\alpha$ such that a sufficiently high level uncertainty on the linear dynamics (typically related to the level of uncertainty in the identification procedure used to identify these dynamics) is permitted by the circle criterion.

5. Closed-loop behaviour

In this section, the closed-loop behaviour of the variable-gain controlled optical storage drive will be investigated for a range of the control design parameters δ (the dead-zone length) and α (the additional gain). These parameters are chosen such that the closed-loop system is exponentially convergent. Consequently, stability is guaranteed and the steady-state performance of the control design can be assessed in a unique fashion. Here we adopt the perspective of periodic disturbances, which will, due to the convergence property, induce unique, globally asymptotically stable periodic responses of the same period time.

The periodic responses of the closed-loop system are evaluated in two ways: firstly using the shooting method and the

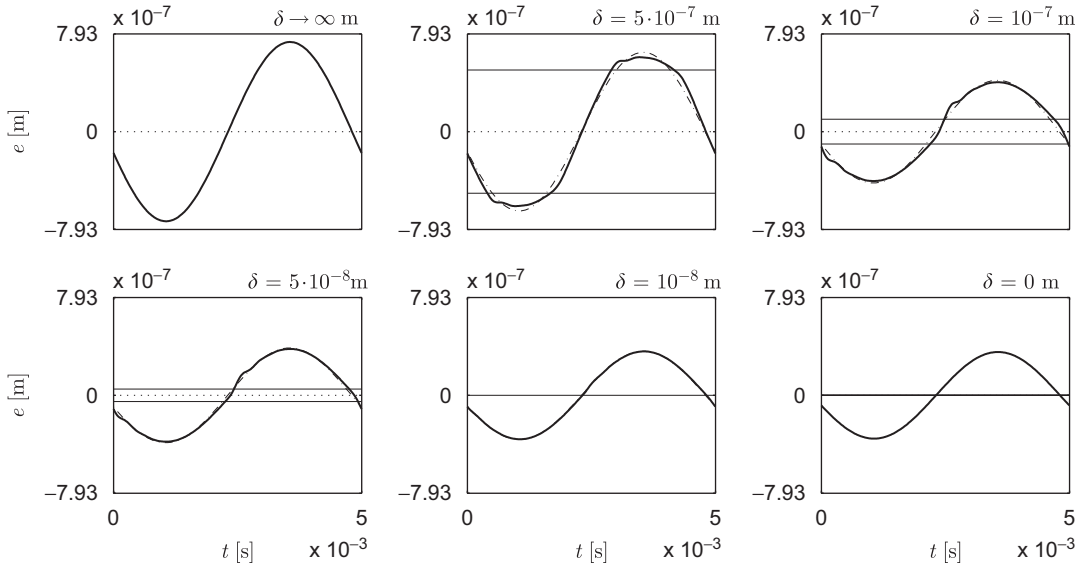

Fig. 6. Closed-loop response $e(t)$ to a harmonic disturbance for a decreasing dead-zone length δ ($\alpha = 1$, $Q = 10^{-5}$ m and $\Omega/(2\pi) = 200$ Hz); simulation (bold lines), describing function approximation (dash-dot lines).

path-following method (Parker & Chua, 1989) to numerically compute the periodic responses of the full nonlinear system and, secondly, using a describing function approximation. For a more detailed derivation of the describing function of the variable-gain element, see Heertjes et al. (2006). Response approximation using describing functions is pursued for reasons of numerical efficiency in evaluating performance for a wide range of the parameters α and δ and for a range of excitation frequencies and amplitudes. It will be shown that the describing function approximation is also accurate for the system under investigation.

The harmonic disturbance is denoted by q: $q(t) = Q\sin(\Omega t)$. In Fig. 6, the periodic error signal $e(t)$ is depicted for $\alpha = 1$, $Q = 10^{-5}$ m and $\Omega/(2\pi) = 200$ Hz and for a decreasing dead-zone length δ. Note that for $\alpha = 1$ the closed-loop system is exponentially convergent, for all δ, and that Fig. 6 depicts the unique globally asymptotically stable periodic steady-state solutions (with a frequency of 200 Hz). The upper left figure relates to $\delta \to \infty$ (the low-gain linear control design) and the lower right figure relates to $\delta = 0$ (the high-gain linear control design). In both designs no gain-switching occurs and the response of such linear control systems is purely harmonic. The intermediate figures express results for various variable-gain designs, where the responses are no longer harmonic (though periodic with the period time of the disturbance). The horizontal lines express the dead-zone length δ and Fig. 6 shows that the error is attenuated when the controller applies higher gains for errors beyond the dead-zone length. Moreover, the results of simulations with the full nonlinear model and results of the describing function approximation are shown. Clearly, the describing function approximation is sufficiently accurate. Finally, Fig. 6 may lead to the conclusion that the high-gain linear design is favourable since it results in the lowest tracking error response for the low-frequency disturbance of 200 Hz. However, the higher linear gain implies a deterioration of the measurement noise sensitivity at higher frequencies with respect to the low-gain linear design. The choice of the dead-zone length in the variable-gain design provides additional design freedom in weighting the performance in terms of low-frequency tracking and the performance in terms of high-frequency measurement noise sensitivity depending on the disturbance characteristic at hand.

In order to quantify this trade-off, simulations are performed for a whole range of excitation frequencies Ω. To enhance the physical meaning of the choice of the dead-zone length, we introduce a scaled dead-zone length $\Delta = \delta/Q$. It can easily be shown that the dependency of the scaled position of the lens p/Q and the scaled error e/Q on the parameters δ and Q can be characterised by a dependency on only one parameter: $\Delta = \delta/Q$. In Fig. 7, the results of these simulations are depicted for $\alpha = 1$. In the upper figure the infinity-norm of the periodic error signal (scaled by Q) is plotted against the disturbance frequency. It is important to note that the infinity-norm of the error is crucial in the performance of the optical storage drive, since the read-out will be terminated when the absolute value of the error becomes larger than the half track width; the latter criterion is related to the servo-error reconstruction mechanism using an extended S-curve (Stan, 1998). In Fig. 7, results for the low-gain linear control design ($\Delta \to \infty$), the high-gain linear design ($\Delta = 0$) and several variable-gain control designs are plotted. For the linear control designs, the upper figure of Fig. 7 merely depicts the absolute value of the sensitivity function $S(\mathrm{j}\Omega) = 1/(1 + H_P(\mathrm{j}\Omega)H_C(\mathrm{j}\Omega))$ and the lower figure of Fig. 7 merely depicts the absolute value of the complementary sensitivity function $T(\mathrm{j}\Omega) = H_P(\mathrm{j}\Omega)H_C(\mathrm{j}\Omega)/(1 + H_P(\mathrm{j}\Omega)H_C(\mathrm{j}\Omega))$. Clearly, for low frequencies the high-gain linear design exhibits better disturbance rejection properties than the low-gain linear design. However, in accordance with

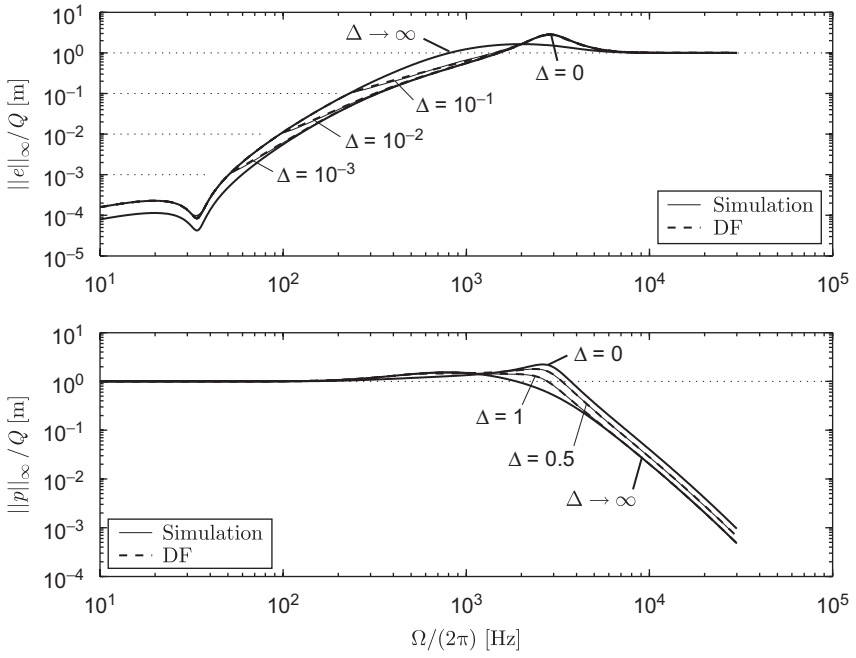

Fig. 7. Generalized sensitivity and complementary sensitivity with $\alpha = 1$ (DF = describing function).

the fact that $S(\mathrm{j}\Omega) + T(\mathrm{j}\Omega) = 1$, $\forall \Omega \in \mathbb{R}$, the low-gain linear design achieves a lower high-frequency noise amplification. For the variable-gain control design we will call the function in the upper plot of Fig. 7 the *generalised sensitivity function* and it expresses both frequency and amplitude dependency. This amplitude dependency can be recognised in the fact that if the disturbance amplitude Q becomes larger, the scaled dead-zone length $\Delta = \delta/Q$ becomes smaller, which induces different closed-loop behaviour. The behaviour of the variable-gain design equals that of the low-gain linear design for $\|e\|_\infty < \delta$. Beyond that level the results of the variable-gain design differ from that of the low-gain linear design.Once the error response of the variable-gain controlled system is such that it spends most of its time outside the dead-zone, the results will resemble that of the high-gain linear design. Consequently, the variable-gain design improves the low-frequency rejection properties with respect to the low-gain linear design ($\Delta \to \infty$); however, it can never improve upon the low-frequency disturbance rejection properties of the high-gain linear design ($\Delta \to 0$). In the lower plot of Fig. 7, the infinity-norm of the periodic lens displacement signal (scaled by Q) is plotted against the disturbance frequency. For the linear control designs, this is the complementary sensitivity function $T(\mathrm{j}\Omega)$ and for the variable-gain design we will call this the *generalised complementary sensitivity function*. This figure expresses the superiority of the low-gain linear design in terms of high-frequency (measurement noise) disturbance rejection properties. Moreover, the variable-gain design improves upon the high-frequency disturbance rejection properties of the high-gain linear design.

Fig. 7 expresses the fact that the variable-gain design can negotiate between low-frequency tracking properties and high-frequency measurement noise sensitivity in a way not available to the linear control designs. Of course, the choice for the *best* design (either linear or variable-gain) is largely determined by the actual frequency- and amplitude-range of both the low-frequency vibrations and the high-frequency measurement noise. Moreover, mere visual inspection of the data plotted in Fig. 7 cannot provide a means to discriminate between the designs in this respect. Therefore, a quantitative performance measure accounting for both low-frequency tracking properties and high-frequency measurement noise sensitivity is necessary to support a performance-based control design strategy. Given the disturbances acting on the system, such performance measure should allow to find the control parameters α and δ achieving optimal performance in terms of both low-frequency tracking properties and high-frequency measurement noise sensitivity.

A performance measure based on computed responses allows to discriminate between the different control designs, see Fig. 7. It should be noted that a (conservative) approach towards performance assessment based on merely providing bounds on the response, given bounds on the disturbances, will not allow to discriminate between the different control designs. Namely, the frequency-dependency expressed by Fig. 7 cannot be accounted for and the bound on the response would always be larger (or equal) than the maximum over the frequencies. Clearly, the upper plot in Fig. 7 shows that the difference in the tracking performance of the different designs is prominent in a frequency range significantly separated from the frequencies for which the maximum (generalised) sensitivity is observed. Therefore, the discrimination between the different control designs can best be assessed through these computed responses.

6. Performance assessment

For optical storage drives, satisfactory performance is achieved when the disc read-out is never stopped, given the disturbances acting on the system. A stop in the disc read-out is directly related to the tracking error exceeding the half track width. Therefore, as mentioned before, the infinity norm of the tracking error should play a central role in the performance measure. Two types of disturbances affect this error: low-frequency vibrations of the disc and high-frequency measurement noise. In optical storage drives, generally performance is increased, firstly, by reducing the influence of measurement noise on the lens position and, secondly, by increasing the capability of the lens to follow the desired disc track in the presence of disc vibrations. Performance in terms of a deviation with respect to the desired disc track is then quantified by a weighted sum of the radial position p of the lens under measurement noise and the radial error e resulting from disc vibrations.

We adopt the perspective of exactly computing the unique steady-state responses to disturbances from the specific class of harmonic disturbances and defining the control performance on the basis of these quantitative data. The latter computations are performed efficiently using describing function approximations, see Section 5. The performance in the face of harmonic disturbances is specifically important for optical storage drives since in practice the performance is tested experimentally by constructing so-called 'drop-out-level curves' (Heertjes et al., 2005), which show the level of the harmonic disturbance for which a termination of the disc read-out occurs for a range of disturbance frequencies. It is worth noting that Theorem 1 also allows one to compute bounds on the responses given bounds on arbitrary inputs, see the discussion at the end of Section 4 and Yakubovich (1964). This allows one to consider more general classes of disturbances, however, only yielding a conservative view on performance.

6.1. Disturbance modelling

In this section, the disturbance modelling is discussed in detail. At this point, we revert to the notation introduced in Section 2: r represents disc vibrations and n denotes the measurement noise. Once more, the perspective of harmonic disturbances is taken: $r(t, \Omega_r, Q_r) = Q_r|F_r(\mathrm{j}\Omega_r)|\sin(\Omega_r t)$, $\forall t \in \mathbb{R}$, $\forall \Omega_r \times Q_r \in [\Omega_r^-, \Omega_r^+] \times [Q_r^-, Q_r^+]$ and zero elsewhere, and $n(t, \Omega_n, Q_n) = Q_n|F_n(\mathrm{j}\Omega_n)|\sin(\Omega_n t)$, $\forall t \in \mathbb{R}$, $\forall \Omega_n \times Q_n \in [\Omega_n^-, \Omega_n^+] \times [Q_n^-, Q_n^+]$ and zero elsewhere, where Q_r and Q_n represent the amplitudes of the disc vibrations r and the measurement noise n, respectively. Similarly, Ω_r and Ω_n represent the frequencies of the disc vibrations r and the measurement noise n, respectively. The linear filters $F_r(\mathrm{j}\Omega_r)$ and $F_n(\mathrm{j}\Omega_n)$ enable appropriate frequency weighting. The choice for representing both the shock disturbances and the measurement noise by means harmonic disturbances (with a range of frequencies) is motivated by, firstly, the fact that the sensitivity to shock disturbances is commonly specified in practice through its sensitivity to harmonic disturbances (Heertjes et al., 2005) (in automotive applications engine- and road-induced vibrations are essentially narrow-banded when arriving at the optical storage drive), secondly, the fact that a specific disc defect induces a disturbance in a pronounced frequency band, whereas the entire considered class of disc defects will represent disturbances in a broad frequency range and, thirdly, the benefit of representing both types of disturbances within the same framework.

The variables $e(t, \Omega, Q)$ and $p(t, \Omega, Q)$ denote the error response and the displacement of the lens to a harmonic disturbance with amplitude Q and angular frequency Ω, respectively. Moreover, by $\|e(t, \Omega, Q)\|_\infty = \sup_{t\in[0,T]}\{|e(r(t, \Omega, Q))|\}$, with $T = (2\pi)/\Omega$ being the period time of the disturbance (and of the response), we denote the maximum absolute error occurring on the periodic steady-state solution induced by the periodic disturbance. A similar notation is adopted for p.

The modelling of $r(t, \Omega_r, Q_r)$ is motivated in the following way. According to the drop-out-level curve (Heertjes et al., 2005), the spectral content of radial disc displacements is in the range from 10 to 200 Hz, i.e. $[\Omega_r^-, \Omega_r^+] = [10 \times 2\pi, 200 \times 2\pi]$ rad/s. Moreover, this frequency range of disturbances is particularly of interest for automotive applications in which the suspension dynamics filters higher disturbances frequencies present in the road excitation. The maximum amplitude of the disc vibrations Q_r^+ and the filter $F_r(\mathrm{j}\Omega_r)$ are chosen such that the combination induces the occurrence of a terminated disc readout (commonly called a mute). The occurrence of a mute conforms to the maximum radial error level in optical disc drives. Now, we choose the filter $F_r(\mathrm{j}\Omega_r)$ such that for a maximal disc vibration amplitude of $Q_r^+ = 4 \times 10^{-7}$, the disc readout is terminated for all disturbance frequencies when the low-gain control design is implemented. For the low-gain linear design, $\|e(r(t, \Omega_r, Q_r))\|_\infty$ is related to the disturbance through the low-gain sensitivity function $S_{lg}(\mathrm{j}\omega)$:

$$\begin{aligned}\|e(r(t, \Omega_r, Q_r))\|_\infty &= \|\mathscr{F}^{-1}\{S_{lg}(\mathrm{j}\omega)R(\mathrm{j}\omega, \Omega_r, Q_r)\}\|_\infty \\ &= Q_r|S_{lg}(\mathrm{j}\Omega_r)F_r(\mathrm{j}\Omega_r)|, \end{aligned} \tag{11}$$

where $R(\mathrm{j}\omega, \Omega_r, Q_r) = \mathscr{F}\{r(t, \Omega_r, Q_r)\}$ is the Fourier transform of $r(t, \Omega_r, Q_r)$. By choosing $|F_r(\mathrm{j}\Omega_r)| = |S_{lg}^{-1}(\mathrm{j}\Omega_r)|$, $\forall \Omega_r \in [10 \times 2\pi, 200 \times 2\pi]$, we guarantee that the disc readout is terminated for $Q_r = Q_r^+$, $\forall \Omega_r \in [10 \times 2\pi, 200 \times 2\pi]$. Consequently, we have constructed a maximum disturbance level (higher disturbance levels are of no interest since the disc readout will already be terminated at lower disturbance levels). Note that $|S_{lg}^{-1}(\mathrm{j}\Omega_r)|$ has a low-pass characteristic for $\Omega_r \in [10\times 2\pi, 200\times 2\pi]$, see left figure in Fig. 8. Motivated by the foregoing line of thought, we model the low-frequency disc vibrations according to $r(t, \Omega_r, Q_r) = Q_r|S_{lg}^{-1}(\mathrm{j}\Omega_r)|\sin(\Omega_r t)$, $\forall t \in \mathbb{R}$, $\forall \Omega_r \times Q_r \in [10 \times 2\pi, 200 \times 2\pi] \times [0, 4 \times 10^{-7}]$.

The modelling of $n(t, \Omega_n, Q_n)$ is motivated as follows. We presume the frequency content of measurement noise due to disc defects starts at 3 kHz, see Vidal, Andersen, Stoustrup, and Pedersen (2001) and Helvoirt, Leenknegt, Steinbuch, and Goossens (2004), i.e. $\Omega_n^- = 3 \times 10^3 \times 2\pi$ rad/s. The latter bound is motivated by a disc defect (e.g. a black dot) of maximum size of 0.002 m encountered while reading an outer track of the DVD

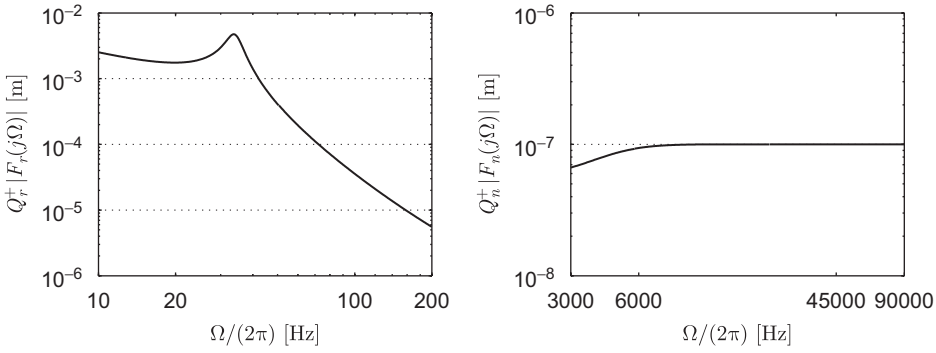

Fig. 8. Design weighting filters and maximum levels of disturbance as a function of frequency.

(at a radius of approximately 0.06 m) while rotating at 15 Hz. In such case the black dot is crossed in approximately 1/3000 s, leading to a lowest disturbance frequency of 3 kHz. The highest frequency at which measurement noise can possibly disturb the output is dictated by half the sample frequency which amounts 45 kHz maximum. Consequently, we define $\Omega_n^+ = 4.5 \times 10^4 \times 2\pi$ rad/s. Measurements are performed to show that, when only measurement noise disturbs the output, generally the measured radial error $\tilde{e}$ does not exceed 10^{-7} m in case the low-gain linear control design is applied. For such a linear control design, the transfer function from n to $\tilde{e}$ is given by the sensitivity function. Using this fact, it is obtained that

$$\begin{aligned}\|\tilde{e}(n(t,\Omega_n,Q_n))\|_\infty &= \|\mathscr{F}^{-1}\{S_{lg}(\mathrm{j}\omega)N(\mathrm{j}\omega,\Omega_n,Q_n)\}\|_\infty \\ &= Q_n|S_{lg}(\mathrm{j}\Omega_n)F_n(\mathrm{j}\Omega_n)|, \end{aligned} \tag{12}$$

where $N(\mathrm{j}\omega,\Omega_n,Q_n) = \mathscr{F}\{n(t,\Omega_n,Q_n)\}$ is the Fourier transform of $n(t,\Omega_n,Q_n)$. To respect the maximum level of $\tilde{e}$ experienced in practice, Q_n^+ is upper bounded through $Q_n^+|S_{lg}(\mathrm{j}\Omega_n)F_n(\mathrm{j}\Omega_n)| = 10^{-7}, \Omega_n \in [3\times10^3\times2\pi, 4.5\times10^4\times2\pi]$ which is guaranteed if we set $Q_n^+ = 10^{-7}$ m and define $|F_n(\mathrm{j}\Omega_n)| = |S_{lg}^{-1}(\mathrm{j}\Omega_n)|$, $\forall\Omega_n \in [3\times10^3\times2\pi, 4.5\times10^4\times2\pi]$, see the right figure in Fig. 8. Motivated by the foregoing reasoning, we model $n(t,\Omega_n,Q_n)$ through $n(t,\Omega_n,Q_n) = Q_n|S_{lg}^{-1}(\mathrm{j}\Omega_n)|\sin(\Omega_n t)$, $\forall t \in \mathbb{R}$, $\forall\Omega_n\times Q_n \in [3\times10^3\times2\pi, 4.5\times10^4\times2\pi]\times[0, 10^{-7}]$. Note that $[\Omega_r^-,\Omega_r^+]\cap[\Omega_n^-,\Omega_n^+] = \emptyset$, which avoids conflicting goals otherwise encountered when both disturbances show a frequency-range overlap.

6.2. Performance measure

The performance measure should reflect the aim to minimise both the effect of the disc vibrations on the tracking error and the effect of the measurement noise on the position of the lens. Moreover, it has been motivated that the infinity-norm of these variables determines whether or not a termination of the disc read-out will occur. Consequently, the performance measure P, which we will call the integral deviation formulation, is formulated as follows:

$$P = \frac{I_r + I_n}{I_r^{\mathrm{ref}} + I_n^{\mathrm{ref}}}, \tag{13}$$

with

$$\begin{aligned} I_r &= \int_{Q_r^-}^{Q_r^+}\int_{\Omega_r^-}^{\Omega_r^+} \|e(r(t,\Omega_r,Q_r))\|_\infty \,\mathrm{d}\Omega_r\,\mathrm{d}Q_r, \\ I_n &= \int_{Q_n^-}^{Q_n^+}\int_{\Omega_n^-}^{\Omega_n^+} \|p(n(t,\Omega_n,Q_n))\|_\infty \,\mathrm{d}\Omega_n\,\mathrm{d}Q_n, \\ I_r^{\mathrm{ref}} &= \int_{Q_r^-}^{Q_r^+}\int_{\Omega_r^-}^{\Omega_r^+} \|e_{ref}(r(t,\Omega_r,Q_r))\|_\infty \,\mathrm{d}\Omega_r\,\mathrm{d}Q_r, \\ I_n^{\mathrm{ref}} &= \int_{Q_n^-}^{Q_n^+}\int_{\Omega_n^-}^{\Omega_n^+} \|p_{ref}(n(t,\Omega_n,Q_n))\|_\infty \,\mathrm{d}\Omega_n\,\mathrm{d}Q_n. \end{aligned} \tag{14}$$

Herein, we accounted for the fact that $[\Omega_r^-,\Omega_r^+]\cap[\Omega_n^-,\Omega_n^+]=\emptyset$ for the disturbance modelling proposed in the previous section. The first integral in the equations in (14), i.e. the integral over $\bar{Q}$, is incorporated to account for the conceivable amplitude dependency inherent to the variable-gain control design. The second integral, i.e. the integral over Ω, is incorporated to account for the frequency dependency of the closed-loop behaviour. Note that in defining (13), (14) it is presumed that the integrands are integrable with respect to Ω and Q, which is guaranteed by the convergence properties of the closed-loop system. The response of an arbitrary reference design is indicated by means of the subscript ref in the denominator of (13). The integral deviation formulation is defined as a relative measure to facilitate the interpretation of its outcome. Namely, if the control design under evaluation (related to the numerator of (13)) and the reference design yield equal performance, a value $P = 1$ is obtained. If, however, $P < 1$, the control design under evaluation yields a better performance than the reference design. For the remainder of this paper the low-gain linear design is chosen to serve as the reference design.

Note that one could also model the disturbances by a parametrised family of signals consisting of multiple harmonics. Then, the same approach can be adopted to assess the performance. Namely, still the convergence properties ensure the existence of a unique and bounded globally asymptotically stable steady-state solution for every bounded disturbance and again this fact allows for a unique performance assessment. However, the performance measure itself will be considerably more complex. Namely, in the case of harmonic disturbances

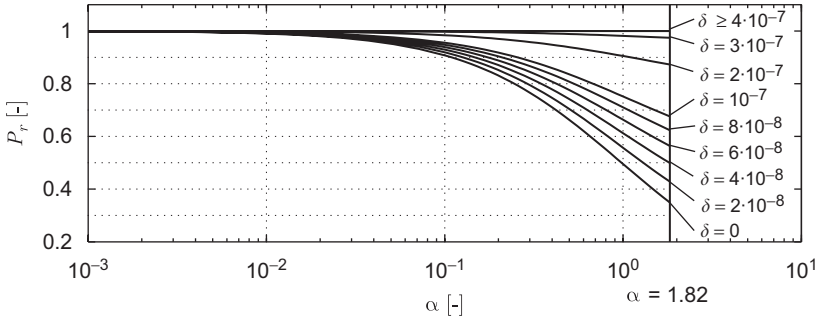

Fig. 9. P_r for a range of linear and variable gain control designs (δ in [m]).

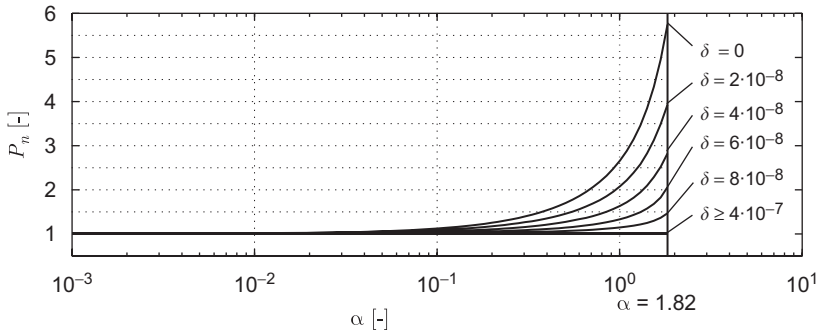

Fig. 10. P_n for a range of linear and variable gain control designs (δ in [m]).

only two parameters (amplitude and frequency) need to be taken into account in the performance measure (see (13), (14)), whereas in the case of multiple harmonics the number of parameters will change accordingly.

6.3. Performance-based control design

Let us now use the performance measure to assess, and compare, the performance of both linear and variable-gain control designs given the type of disturbances described in Section 6.1. In order to illuminate qualitative contributions of improvements/deteriorations with respect to low-frequency disturbance rejection properties and high-frequency measurement noise sensitivity to the performance P, the following quantities are introduced: $P_r = I_r/I_r^{\text{ref}}$ and $P_n = I_n/I_n^{\text{ref}}$. Provided Ω_r^+ is below the bandwidth of the reference design, by means of P_r the conceivable improvement in low-frequency disturbance rejection properties is studied. Furthermore, provided that Ω_n^- is above the bandwidth of the reference design, P_n enables a quantification of the possible deterioration of measurement noise sensitivity. Note that $P \neq P_r + P_n$.

Fig. 9 depicts the value of P_r as a function of α. Herein, $\alpha \in [0, 1.82]$ as to guarantee convergent system properties, see Section 4. Furthermore, P_r is evaluated for several levels of the dead-zone length δ. If $\delta \geqslant 4 \times 10^{-7}$ m, it is obtained that $P_r = 1$, $\forall \alpha \in [0, 1.82]$, because the error due to radial disc displacement is upper-bounded by 4×10^{-7} m, see Section 6.1. Therefore, if $\delta \geqslant 4 \times 10^{-7}$ m, the dead-zone will not be exceeded. For smaller values of δ, $P_r < 1$ $\forall \alpha \in [0, 1.82]$ implying an improvement of low-frequency disturbance rejection properties. The monotonic decrease of P_r with α follows from the fact that we evaluate the radial error merely for frequencies below the bandwidth of the reference design. Not surprisingly, P_r is minimal if (i) $\delta = 0$ m, i.e. for the high-gain linear design, and (ii) $\alpha = 1.82$; hence maximal low-frequency disturbance attenuation is attained.

Fig. 10 depicts the value of P_n as a function of α. For $\delta \geqslant 10^{-7}$ m, it is obtained that $P_n = 1$, $\forall \alpha \in [0, 1.82]$ because the measured radial error resulting from measurement noise is upper-bounded by 10^{-7} m, see Section 6.1. For smaller values of δ, it is obtained that $P_n \geqslant 1$, $\forall \alpha \in [0, 1.82]$, indicating a deterioration of measurement noise sensitivity. The monotonic increase of P_n with α is caused by considering the measurement noise sensitivity only for frequencies above the bandwidth of the reference design. The measurement noise sensitivity is deteriorated to a maximum extent if (i) $\delta = 0$ m hence for the high-gain linear design, and (ii) $\alpha = 1.82$.

Fig. 11 depicts the outcome of (13) evaluated for the disturbances, modelled in Section 6.1, as a function of α. Furthermore, P is evaluated for several levels of the dead-zone length δ. The figure indicates that the performance depends strongly on both α and δ. If $\delta \geqslant 4 \times 10^{-7}$ m, it is obtained that $P = 1$ $\forall \alpha \in [0, 1.82]$. Initially, a reduction of δ will enhance performance because low-frequency disturbance rejection properties are improved whereas the measurement noise sensitivity remains unaltered, see the curves for $\delta \in \{10^{-7}, 2 \times 10^{-7}, 3 \times 10^{-7}\}$ m. For these levels of δ, P decreases monotonically with α and therefore maximum performance, i.e. minimum P, is obtained if $\alpha = 1.82$.

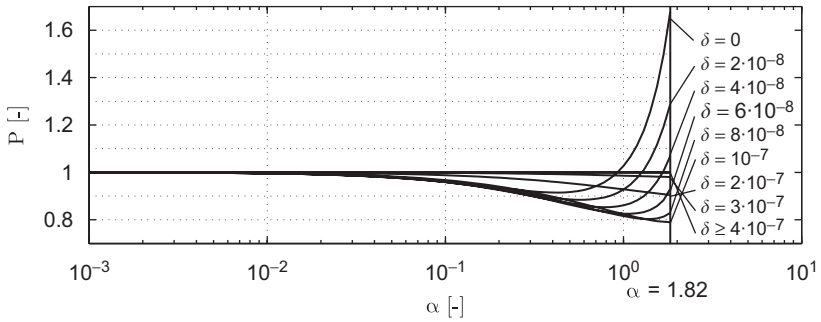

Fig. 11. The performance measure P for a range of linear and variable gain control designs (δ in [m]).

A further decrease of δ results in a deterioration of performance compared to the design with $\delta = 10^{-7}$ m. Namely, if $\delta < 10^{-7}$ m, the measured radial error resulting from measurement noise will exceed the dead-zone length and hence, a deterioration of the measurement noise sensitivity is effected. Consequently, P no longer monotonically decreases with α and therefore, maximum performance is no longer obtained for maximum α. If $\delta \in \{6 \times 10^{-8}, 8 \times 10^{-8}\}$ m, the variable gain control design under evaluation still accomplishes better performance than the reference design for all $\alpha \in [0, 1.82]$. Note that the level of the dead-zone length on the boundary between performance deterioration and improvement strongly depends on the (relative) level of the two types disturbances (shock disturbances and disc defects). However, for $\delta \in \{0, 2 \times 10^{-8}, 4 \times 10^{-8}\}$ m there exist values for α for which $P > 1$, implying a deterioration of the performance compared to the low-gain linear design. For these levels of δ, the improvement in low-frequency disturbance rejection properties is canceled by the deterioration of the measurement noise sensitivity. Therefore, for smaller levels of δ, the increase of the gain α within the range for which convergence is guaranteed, does not lead to an improved performance. In order not to arrive at a worsening of performance compared to the low-gain linear design for these levels of δ, one must select α carefully.

Depending on the combination of α and δ, the variable gain control design can outperform both the low-gain and the high-gain linear design. Given the performance measure (13), the weighting filters in Fig. 8 and the disturbance modelling proposed in Section 6.1, Fig. 11 clearly shows that nonlinear control can prevail over linear control.

The proposed performance-based design strategy allows to compute settings of the control parameters α and δ that guarantee 'optimal' performance given the plant and disturbance model. In practice, the sensitivity of the optimality of such control settings with respect to model uncertainties is an important issue. However, the dynamics of the system under study can be modelled with high accuracy by exploiting simple frequency-domain identification procedures, see, for example, Heertjes et al. (2006). Moreover, if large deviations in the controlled mechanics would occur, a redesign of the nominal (low-gain) control design would be in effect in practice aiming at the same type of nominal closed-loop dynamics (e.g. in terms of nominal bandwidth).

7. Conclusions

In this paper, a variable-gain control design for optical storage drives is studied from a control performance perspective. The variable-gain strategy is adopted to overcome well-known linear control design trade-offs between low-frequency tracking properties and high-frequency noise sensitivity.

The contribution of this paper lies in the following aspects. Firstly, a convergence-based control design is proposed, which guarantees stability of the closed-loop system and a unique bounded steady-state response for any bounded disturbance. These favourable properties, induced by convergence, allow for a unique steady-state performance evaluation of the control system. Secondly, technical conditions for exponential convergence are proposed for the variable-gain controlled system. Thirdly, a quantitative performance measure, taking into account both low-frequency tracking properties and high-frequency measurement noise sensitivity, is proposed to support the design and tuning of the nonlinear (non-smooth) control design.

The proposed performance measure is based on the computed steady-state responses to a class of harmonic disturbances, which allows for an accurate performance comparison between different control designs. Such a performance measure is consistent with industrial performance specifications for optical storage drives which are given in terms of the level of harmonic disturbances for which the data read-out is terminated. The convergence conditions together with the performance measure jointly constitute a design tool for tuning the parameters of the variable-gain controller. The resulting design is shown to outperform linear control designs. The latter statement is based on the steady-state behaviour of the control system under harmonic excitation and is supported by measurements in Heertjes et al. (2006).

As a final remark, the trade-off between low-frequency tracking properties and high-frequency measurement noise sensitivity is not unique for optical storage drives but can be recognised in a wide variety of motion control systems, such as pick and place machines, robots, etc. As a consequence, the method towards performance assessment proposed here can support the design of variable-structure controllers for other applications as well.

The discriminative nature of the performance evaluation can be further improved by future work on enhanced disturbance modelling.

References

Angeli, D. (2002). A Lyapunov approach to incremental stability properties. *IEEE Transaction on Automatic Control*, *47*, 410–421.

Armstrong, B., Neevel, D., & Kusid, T. (2001). New results in NPID control: Tracking, integral control, friction compensation and experimental results. *IEEE Transactions on Control Systems Technology*, *9*(2), 399–406.

Armstrong, B. S. R., Gutierrez, J. A., Wade, B. A., & Joseph, R. (2006). Stability of phased-based gain modulation with designer-chosen switch functions. *International Journal of Robotics Research*, *25*, 781–796.

Bittanti, S., Dell'Orto, F., Di Carlo, A., & Savaresi, S. M. (2002). Notch filtering and multirate control for radial tracking in high-speed DVD-players. *IEEE Transactions on Consumer Electronics*, *48*(1), 56–62.

Demidovich, B. P. (1967). *Lectures on stability theory*. Moscow: Nauka, (in Russian).

Freudenberg, J., Middleton, R., & Stefanopoulou, A. (2000). A survey of inherent design limitations. In: *Proceedings of the American control conference* (pp. 2987–3001). Chicago, Illinois, USA.

Fromion, V., Monaco, S., & Normand-Cyrot, D. (1996). Asymptotic properties of incrementally stable systems. *IEEE Transactions on Automatic Control*, *41*, 721–723.

Fromion, V., & Scorletti, G. (2002). Performance and robustness analysis of nonlinear closed-loop systems using μ_{nl} analysis: Applications to nonlinear PI controllers. In: *Proceedings of the 41st IEEE conference on decision and control* (pp. 2480–2485). Las Vegas, Nevada, USA.

Fromion, V., Scorletti, G., & Ferreres, F. (1999). Nonlinear performance of a PI controlled missile: An explanation. *International Journal of Robust and Nonlinear Control*, *9*, 485–518.

Heertjes, M. F., Cremers, F., Rieck, M., & Steinbuch, M. (2005). Nonlinear control of optical storage drives with improved shock performance. *Control Engineering Practice*, *13*(10), 1295–1305.

Heertjes, M. F., Pastink, H. A., van de Wouw, N., & Nijmeijer, H. (2006). Experimental frequency-domain analysis of nonlinear controlled optical storage drives. *IEEE Transactions on Control Systems Technology*, *14*(3), 389–397.

Heertjes, M. F., & Sperling, F. B. (2003). A nonlinear dynamic filter to improve disturbance rejection in optical storage drives. In: *Proceedings of the 42nd conference on decision and control* (pp. 3426–3430). Maui, Hawaii, USA.

Heertjes, M. F., & Steinbuch, M. (2004). Stability and performance of a variable gain controller with application to a DVD storage drive. *Automatica*, *40*, 591–602.

Helvoirt, J., Leenknegt, G. A. L., Steinbuch, M., & Goossens, H. J. (2004). Classifying disc defects in optical disc drives by using time-series clustering. In: *Proceedings of the American control conference* (pp. 3100–3105). Boston, Massachusetts, USA.

Jiang, F., & Gao, Z. (2001). An application of nonlinear PID control to a class of truck ABS problems. In: *Proceedings of the 40th IEEE conference on decision and control* (pp. 516–521). Orlando, Florida, USA.

Lohmiller, W., & Slotine, J.-J. E. (1998). On contraction analysis for nonlinear systems. *Automatica*, *34*, 683–696.

Parker, T. S., & Chua, L. O. (1989). *Practical numerical algorithms for chaotic systems*. Berlin: Springer.

Pavlov, A., Pogromsky, A., van de Wouw, N., & Nijmeijer, H. (2004). Convergent dynamics, a tribute to Boris Pavlovich Demidovich. *Systems and Control Letters*, *52*, 257–261.

Pavlov, A., van de Wouw, N., & Nijmeijer, H. (2005). *Uniform output regulation of nonlinear systems: A convergent dynamics approach*. Boston: Birkhäuser. (in Systems & Control: Foundations and Applications (SC) series).

Stan, S. G. (1998). *The CD-ROM drive, a brief system description*. Dordrecht: Kluwer Academic Publishers.

Vidal, E., Andersen, P., Stoustrup, J., & Pedersen, T.S. (2001). A study on the surface defects of a compact disk. In: *Proceedings of the IEEE conference on control applications* (pp. 101–104). Mexico City, Mexico.

Yakubovich, V. A. (1964). The matrix inequality method in the theory of the stability of nonlinear control systems—I. The absolute stability of forced vibrations. *Automation and Remote Control*, *7*, 905–917.

Nathan van de Wouw (born, 1970) obtained his M.Sc. and Ph.D. degree in Mechanical Engineering from the Eindhoven University of Technology, Eindhoven, the Netherlands, in 1994 and 1999, respectively. From 1999 until now he has been affiliated with the Department of Mechanical Engineering of the Eindhoven University of Technology in the group of Dynamics and Control as an assistant professor. In 2000, Nathan van de Wouw has been working at Philips Applied Technologies, Eindhoven, The Netherlands, and, in 2001, he has been working at the Netherlands Organisation for Applied Scientific Research (TNO), Delft, The Netherlands. He has held a visiting research position at the University of California Santa Barbara, U.S.A., in 2006/2007. Nathan van de Wouw has published 26 publications in international journals, 5 book contributions and 40 refereed proceedings contributions at international conferences. Recently he published the book 'Uniform Output Regulation of Nonlinear Systems: A convergent Dynamics Approach' with A.V. Pavlov and H. Nijmeijer (Birkhauser, 2005). His current research interests are the analysis and control of non-smooth systems and networked control systems.

Erik Pastink was born in Amsterdam, The Netherlands, in 1978. He received the M.Sc. degree in mechanical engineering (cum laude) from Eindhoven University of Technology, Eindhoven, The Netherlands, in 2004. The work for his thesis, entitled "Stability and Performance of Variable Gain Controlled Optical Storage Drives," was carried out at Philips Applied Technologies. Currently, he is a Mechatronics Design Engineer with the R&D Department, Océ Technologies, Venlo, The Netherlands. Mr. Pastink received the Unilever Research Award in 2005 and the Royal Institution of Engineers' Control Award in 2005.

Marcel Heertjes was born in Goes, the Netherlands in 1969. He received both his M.Sc. and Ph.D. degree in mechanical engineering from the Eindhoven University of Technology in 1995 and 1999, respectively. In 2000, he joined the Philips Centre for Industrial Technology in Eindhoven. Since 2007 he is with ASML, Mechatronics Development, in Veldhoven and with the control system technology group at the Eindhoven University of Technology. He has published over thirty refereed papers and received over ten patents. His main field of interest is the control of industrial motion systems with special attention for variable gain control systems and learning control.

Alexey Pavlov (born 1976) received the M.Sc. degree (cum laude) in Applied Mathematics from St. Petersburg State University, Russia in 1998. In 1999 he was a part-time researcher in the group Control of Complex Systems at the Institute for Problems of Mechanical Engineering, Russian Academy of Sciences. In 2000 he was a visiting research scientist at Ford Research Laboratory, Dearborn, USA. In 2004 he received the Ph.D. degree in Mechanical Engineering from Eindhoven University of Technology, The Netherlands. Currently he holds an Assistant Professor position at the Norwegian University of Science and Technology, Department of Engineering Cybernetics. Alexey Pavlov has co-authored 34 journal and conference publications, 2 patents and a monograph "Uniform output regulation of nonlinear systems: a convergent dynamics

approach" (Birkhauser, 2005). His research interests include control of nonlinear and hybrid systems, nonlinear output regulation theory, convergent systems and cooperative control.

Henk Nijmeijer (1955) obtained his M.Sc. and Ph.D. degrees in Mathematics from the University of Groningen, Groningen, the Netherlands, in 1979 and 1983, respectively. From 1983 until 2000 he was affiliated with the Department of Applied Mathematics of the University of Twente, Enschede, the Netherlands. Since, 1997 he was also part-time affiliated with the Department of Mechanical Engineering of the Eindhoven University of Technology, Eindhoven, the Netherlands. Since 2000, he is a full professor at Eindhoven, and chairs the Dynamics and Control section. He has published a large number of journal and conference papers, and several books, including the 'classical' Nonlinear Dynamical Control Systems (Springer Verlag, 1990, co-author A.J. van der Schaft), with A. Rodriguez, Synchronization of Mechanical Systems (World Scientific, 2003), with R.I. Leine, Dynamics and Bifurcations of Non-Smooth Mechanical Systems (Springer-Verlag, 2004), and with A. Pavlov and N. van de Wouw, Uniform Output Regulation of Nonlinear Systems (Birkhauser 2005). Henk Nijmeijer is editor-in-chief of the Journal of Applied Mathematics, corresponding editor of the SIAM Journal on Control and Optimization, and board member of the International Journal of Control, Automatica, Journal of Dynamical Control Systems, International Journal of Bifurcation and Chaos, International Journal of Robust and Nonlinear Control, and the Journal of Applied Mathematics and Computer Science. He is a fellow of the IEEE and was awarded in 1990 the IEE Heaviside premium.